Biomedicine and Chemical Sciences 1(4) (2022) 270-277

36-BCS-1087-284

Content lists available at:
https://journals.irapa.org/index.php/BCS/issue/view/15

Biomedicine and Chemical Sciences

Journal homepage: https://journals.irapa.org/index.php/BCS

Novel Semi-Automated Design for Determination of Iron in Water using Smartphone Camera Complementary Metal-Oxide-Semiconductor (CMOS) Biosensor as a Detector Device

Hassan Hadi Kadhim, Mustafa Abdulkadhim Hussein*

Department of Chemistry, Faculty of Science, University of Kufa – Iraq

ARTICLE INFO

Article history:
Received on: July 26, 2022
Revised on: August 06, 2022
Accepted on: August 07, 2022
Published on: October 01, 2022

Keywords:
1.10-Phenanthroline
Bio sensor
Hydroxylamine
Iron (II) sulfate heptahydrate
Smart-phone
Spectrophotometry

ABSTRACT

In this research, a new method was used to determine the amount of iron in water, by using the colour biosensor of the smart-phone device as a biosensor for the chromatic intensity of the samples images that are examined through a program (colour meter) downloaded to the phone. The concentration of the samples is measured from the value of the basic colours (red, green, blue) (RGB) for recorded video from a device (Galaxy J7 prime 2). An accessory for the mobile device is designed from plastic (black acrylic). In the form of a dark box from the inside equipped with a flow cell and a mirror reflecting the flash light emitted by the mobile device and a green filter complementing the red colour, and a micro switch connected to a smart-phone device via earphones, and the device is attached to the accessory by the device case. The calibration curve for this method was in the range of mg/L (1-8), the correlation coefficient (R^2) was equal to (0.999), the limit of detection was in the amount of (0.2) mg/L, and the relative standard deviation (RSD%) for the concentration was (4) mg/L, for which the examination was repeated (10) times, and its value was (0.6 %), and the recovery value (Recovery%) was equal to (101.5 %).

1. Introduction

Due to lower prices and the growing demands of multimedia applications, digital smart cameras are currently spreading quickly. There are still improvements to be achieved with two key image sensor technologies: charge-fixed devices (CCDs) and complementary metal-oxide-semiconductor (CMOS) biosensors. (CCDs) have traditionally been the most used image-sensor technology. However, ongoing developments in (CMOS) technology for processors and storage have made (CMOS) bio sensor arrays a competitive alternative to the widely used CCD sensors. As a result, (CMOS) image bio sensors were approved for use in a number of high-volume products, including webcams, smartphones, and medications. With the help of new machinery, it is now feasible to combine a huge number of very-large measure integration (VLSI) electronics into a single defect, which significantly lowers the cost, power consumption, and size (Durini, 2019). By exploiting these advantages, innovative CMOS sensors have been developed (Ginhac, 2014).

When semiconductor, optics, and packing technology developed to enable the development of tiny cameras, camera phones became commonplace. Mobile phones quickly took off to the point where hundreds of millions of users kept them at arm's length and used them almost nonstop. Around 1999, the combination of these tiny cameras and mobile phones created the largest and fastest-growing imaging market in history, with several billion-camera phones in circulation and producing reams of photos and reams of video paperclips. The majority of people worldwide had their first experience capturing images with a

***Corresponding author:** Mustafa Abdulkadhim Hussein, Department of Chemistry, Faculty of Science, University of Kufa – Iraq
E-mail: **mustafa.rabeea@uokufa.edu.iq**

How to cite:

Hussien, M. . A., & Kadhim, H. . H. (2022). Novel Semi-Automated Design for Determination of Iron in Water using Smartphone Camera Complementary Metal-Oxide-Semiconductor (CMOS) Biosensor as a Detector Device. *Biomedicine and Chemical Sciences, 1*(4), 270-277.

DOI: **https://doi.org/10.48112/bcs.v1i4.284**

camera phone. The size of the mobile market necessitates the manufacture of about 600,000 sensors each day, 2 billion annually, or over 200,000 300-mm wafers every month. Imagine the number of processor chips or display devices in the world and the growth rate of those.

Each will be connected to at least one image biosensor (Levin & Stevens, 2014). Smartphone –based sensing devices are gaining momentum and have opened new avenues towards next generation point-of care sensing and bio sensing application (Roda, et al., 2016). The flexibility to incorporate signal distribution at the focus plane lowered to the pixel close is another major benefit of (CMOS) image sensors. Dispensation units can be understood at chip level using a system-on-chip approach, at column level by dedicating processing elements to one or more columns, or at pixel level by integrating a specific processing unit in both pixel and column levels as (CMOS) image sensors scale to 0.13um processes and below (El Gamal, Eltoukhy & Sensors, 2005). The goal of researchers has always to achieve greater performance imaging systems built on (CMOS) technology in order to fiercely compete with (CCD) equipment. As a result, there have been numerous rumors regarding ways to improve the fill-factor with low control consumption, low power operation, low noise, high imaging speed, and high active range.

Additionally, research on other subjects, such pixel contour improvement, is still in its infancy (Shcherback & Yadid-Pecht, 2003). SOI substrate with pixels (Zhang, et al., 1999), high determination (Bigas, et al., 2006), APS with flexible resolution (Zhou, Pain & Fossum, 1998; Coulombe, Sawan & Wang, 2000), Self-correcting (Audet & Chapman, 2001; Koren, Chapman, & Koren, 2000) and for low sunlit (Goy, et al., 2001; Croft, 1999), etc. The (CMOS) imager development, on the other hand, has led to the creation of new applications. Enhancements have been made to motorized applications, image for mobile or stationary phones, processor video, space, medical, numerical photography, and 3D applications. With so many applications blowing out, (CMOS) technology innovated on two facades in 2000: ultrahigh speed, big arrangement imaging on the high end, and sensors for computers and booth phones on the low end (Fossum & Krymski, 2000). New developments in smartphone technology have pushed the arenas of chemical and biological detecting into a wide range of analyzes (Christodouleas, ET AL., 2015).

The primary component used in a smartphone is the camera that allows color images to be measured using colorimetric or photometry, and chromatography is a fundamental chemical technique that makes use of equipment like spectrometers or test strip readers that are specially made for this function. Chemists typically use color to monitor reactions, but they also need to employ equipment to obtain more quantitative information. Only if the image that is captured can be measured can smartphone technology aid chemists in their chromatography procedures. Using smartphone spectrophotometers based on common photos and the Beer-Lambert Law to assess the absorption of colored liquids is one technique to achieve this goal (Iqbal & Eriksson, 2013). In this study, a new method included iron determination in water by primary color analysis (RGB) of video recorded for samples by smartphone.

2. Materials and Methods

2.1. Chemicals

All solutions of chemicals used in water were prepared the degree of analytical reagent. Iron (II) sulfate heptahydrate solution ($FeSO_4.7H_2O$) was prepared at a concentration of (0.00017 M) by dissolving (0.01 g) in (200 mL) of water .then added 1 mL from Concentrated sulfuric acid completes the volume to 200 mL and this solution is its concentration 10 ppm .A solution of 1.10-phenanthroline monohydrate ($C_{12}H_8N_2 . H_2O$) is prepared by taking 0. 1 g and dissolving it in 100 mL distilled water with simple heating to complete the dissolution process. A hydroxylamine hydrochloride solution ($NH_2OH.HCl$) is prepared by taking 5 g and dissolving it in 50 mL distilled water. Sodium acetate (CH_3COONa) solution is prepared by taking 5 g and dissolving it in 50 mL distilled water.

2.2. Equipment

1. UV-Visible Spectrophotometer ,EMC-11UV, Emclab, Germany.(single Beam)
2. Electric Balance, BP 301S, Sartorius, Germany
3. Heater Magnetic Stirrer, EQ-10198, China
4. Mobile device (Galaxy J 7 Prime 2). China
5. Micro switch, Singapore

2.3. Methods Used in Measurement

Two different methods of measurement were used:

The first method: is one of the traditional methods for the determination of iron in water using a device (Spectrophotometer). The second method: it is a new method that relies on the use of the colour bio sensor on the smartphone device (Galaxy J 7 Prime 2) through a program that is downloaded on the smartphone device, which analyses the colour intensity of the main colours (RGB) of the captured images.

2.3.1. Traditional Method Using the Device (Spectrophotometer)

Spectrophotometers measure the amount of light absorbed by a sample. All coloured solutions absorb visible light and can, therefore, be analysed with a spectrophotometer. This experiment uses a spectrophotometer to determine the concentration of iron (II), This method is based on the formation of a red complex between iron (II) and the compound 1.10-Phenanthroline and this method is very sensitive to the determination of iron by the molecular absorbance of this compound $\{(C_{12}H_8N_2)_2Fe\}^{+2}$, This complex absorbs light in the visible region rather strongly with a maximum absorbance occurring around 508 nm.

There are several steps that must be taken when conducting tests with the (Spectrophotometer) device, which are (Haris, 2003; Marczenko & Balcerzak, 2000):

1. The standard solution of iron (II) is prepared as follows:0.01 g iron sulfate heptahydrate ($FeSO_4.7H_2O$) is taken and dissolved in water in 20 mL beaker, then added 1 mL from concentrated sulfuric acid completes

the volume to 200 mL and this solution is its concentration 10 ppm

2. Prepare standard solution of the following concentration: 0, 1 , 2, 3 ,4, 6 , and 8.0 ppm

3. A solution of 1.10-phenanthroline monohydrate is prepared by taking 0. 1 g and dissolving it in 100 mL distilled water with simple heating to complete the dissolution process

4. A hydroxylamine solution is prepared by taking 5 g and dissolving it in 50 mL distilled water

5. Sodium acetate solution is prepared by taking 5 g and dissolving it in 50 mL of distilled water

2.3.1.1. The Calibration Curve

Within the optimal operating conditions, the working and the standard solutions were prepared by serial dilution of solution to find the standard curve and determination the limit of detection (LOD) The relative standard deviation (RSD), recoveries and regression coefficient of this reaction. After completing the calibration process for the (Spectrophotometer), the results were confirmed by drawing a calibration curve between absorbance and concentration, and the value of the correlation coefficient (R2) for the calibration curve was equal to (0.997) and it is considered a good value from a statistical point of view (Figure 1).

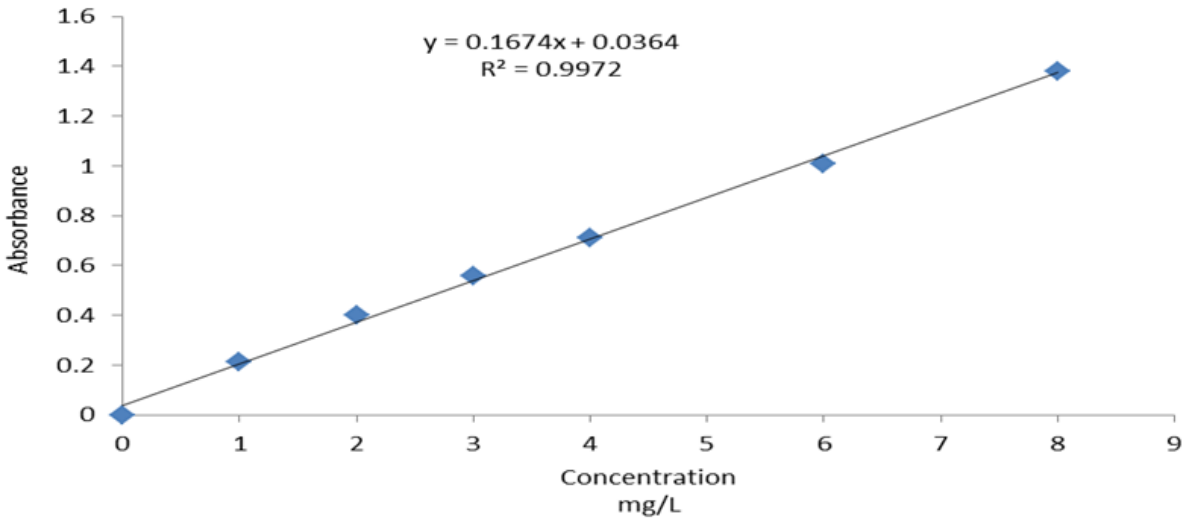

Fig. 1. Diagram of the calibration curve between the absorbance and concentration of the (Spectrophotometer)

3. Results and Discussion

3.1. Sample Chamber Design and RGB Measurement Method Using a Smartphone

A rectangular box is designed from plastic (black acrylic) with a length of 6 cm, a width of 4 cm, and a height of 6 cm, as in Figure 2, and two holes were made in the box. A hole for the entry of light resulting from the flicker the phone (flash) and other for video recording of the models. Three holes were made in the cover of the box. The first was through which the solution was injected, and the second was through which the reagent was injected, where each of them was connected to a tube. The distance between the two tubes was at the meeting point of the solution with the detector (2.5 cm), and from it, the tube was connected to the entrance to the flow cell. The third was where the micro switch was installed. It was a key mechanical device used to cut off or divert current from one path to another within the circuit as in Figure 2 (a). There was an opening at the bottom of the box for the exit of the solution, through a pipe connected to the other entrance of the flow cell. The size of the injected model was (2ml) for each model and the height of the flow cell was (3 cm). The cell was painted black from the inside and outside except for two ports for the entry and exit of light in the form of a small circle representing the diameter and amount of the cell tubes (1.8 mm) as in Figure2 (b). Inside the black box there was a reflective mirror that reflected the flashing light of the phone on one of the light ports of the flow cell near the mirror so that the video was recorded from the other port of the cell. The distance between the light port of the flow cell and the mirror was within (4.5 cm), there was also a small piece of green glass (complementary to the red color) attached to the entry port of the light into the flow cell. As in Figure 3, the phone is fixed to the black box by means of the device case, as in Figure 2 (d).

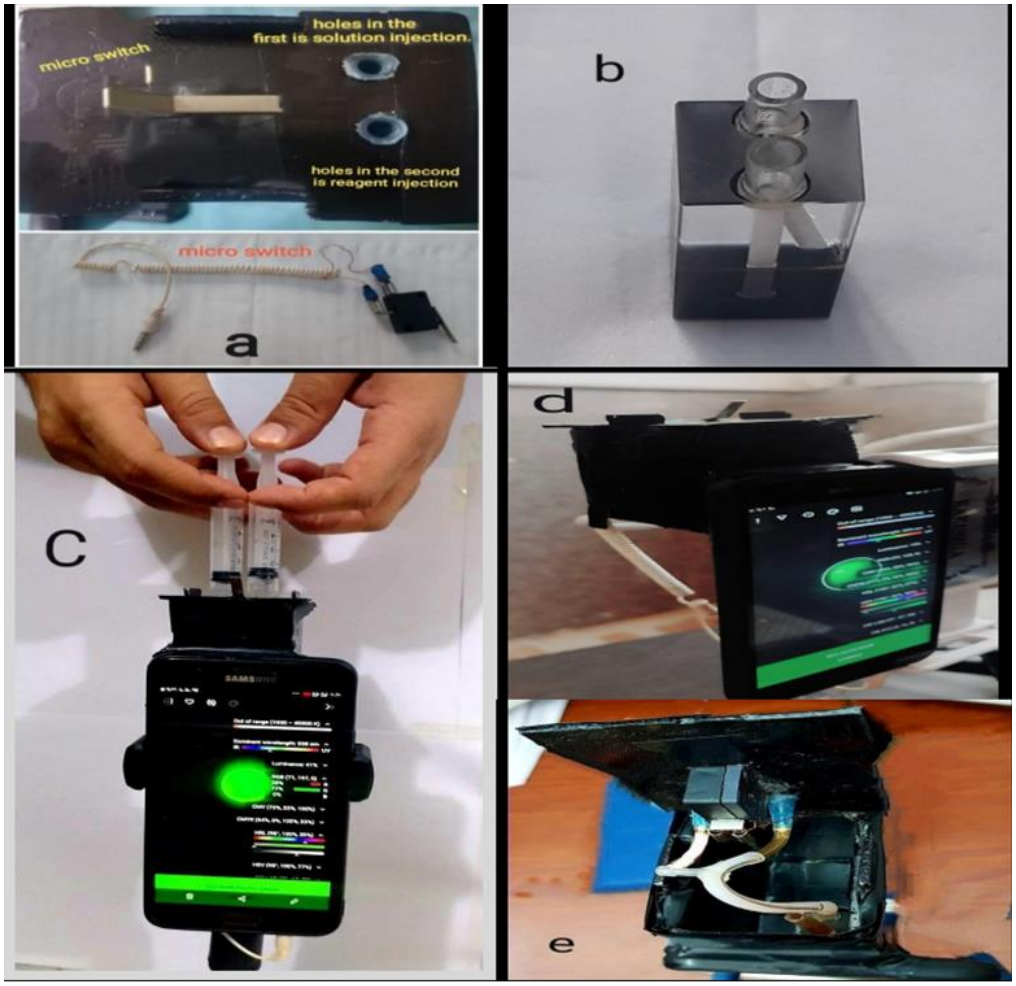

Fig. 2. The parts of the box attached to the smartphone and the way it works (a) Box cover and micro switch. (b) Flow cell. (c) Injection of samples into the flow cell. (d) The telephone set is installed on the Black box by device case. (e) The black box from the inside.

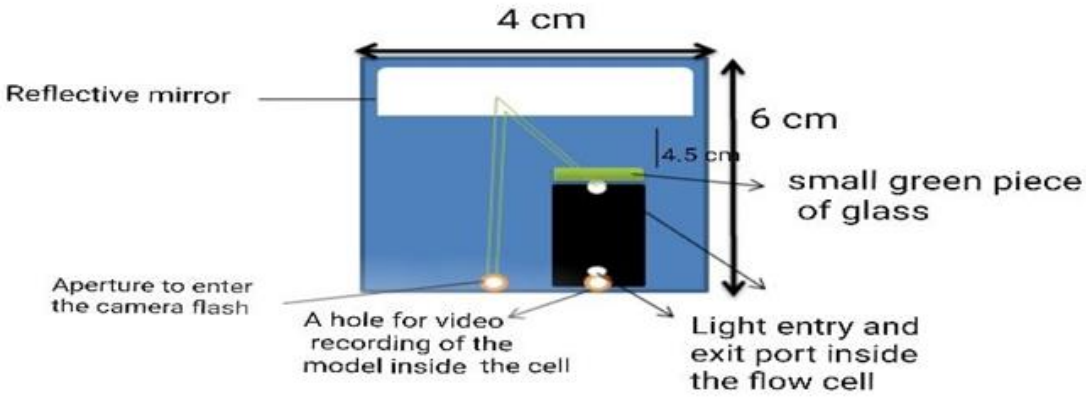

Fig. 3. Diagram of the design of a box attached to a smartphone device.

The steps involved in the (determination of iron in water) process of the (spectrophotometer), which were explained in the second chapter title (2.3.1), are the same steps used in the (RGB) method with a smartphone. After that, we withdraw an amount of the solution and the reagent, and the solutions are manually injected through Hamilton syringes using the sequential method, where both are transferred through the tube to the flow cell installed in the black box as in Figure 2 (c). We install the smartphone device on the front of the box so that the camera hole of the phone applies to the black box slot designated to see the light port of the flow cell, and the flash slot of the device applies to the other slot in the box designated for entering the flash light. During the injection process, we press the

micro switch which is connected to a smartphone device via earphones, to record the video of the sample inside the flow cell, and after 10 s of time have passed, we press again on the piston to stop the video recording and save it, and a screenshot is taken at the 10 s time of the recorded video, and then analyze the colors of the image using the (Color picker) program to find the (RGB) value for recorded video, which represents the emitting light in Beer-Lambert's law, after completing each inspection process, the flow cell is cleaned with pure water , and the reflective mirror is clean. We extract the absorbance value of the sample by applying (Beer-Lambert Law) to find the absorbance

$$A = - \text{Log} (I / I^{\circ}) \quad (1)$$

A = absorbance

I = the transmitted light, and represents the (G) value for recorded video of the model.

I° = the incident light, and it represents the (G) value of green light.

We extract the concentration value of the model through the calibration curve that was prepared in advance and the calibration points were fixed for this purpose, through the linear regression equation, which is expressed by the following equation:

$$A = m \times (Conc) \pm b \quad (2)$$

$$Conc = A \pm b / m \quad (3)$$

3.2. Injection Time Study

The injection time was studied, by measuring the absorbance of a concentration of 2 ppm of the solution. A change in the absorption of the solution was observed when the time period gradually increased up to10 s, since the formation of the complex. It was noted that the compound absorption remained constant for a period of time, so 10 s are the preferred time period.

3.3. Reproducibility Study

To ensure the conformity of the results obtained by color density (RGB) by the smartphone, we studied the congruence of the results of tests for (10) duplicate images taken at a concentration of (4) mg/L, and the (RSD) value of the match was (0.6 %) and the recovery value (Recovery) equals (101.5 %), as in Table 1, and Figure 4, below.

Table 1
The congruence results of the RGB method

	Value G	Absorbance	Concentrations measured by chromatic intensity method (mg/L)	RSD%	Recovery%
1	175	0.994	4.078		
2	175	0.994	4.078		
3	174	0.101	4.144		
4	175	0.994	4.078		
5	175	0.994	4.078		
6	175	0.994	4.078	0.60%	101.50%
7	175	0.994	4.078		
8	174	0.101	4.144		
9	175	0.994	4.078		
10	175	0.994	4.078		

Fig. 4. Images of concordance study of concentration 4 mg/L.

3.4. Studying the Detection Limit for the RGB Method

The detection limit represents the least analytical quantity in the substance that can be detected, when measuring the detection limit of the chromatic density (RGB) method, three solutions were prepared with concentrations of 0.2 mg/L, 0.4mg/L, and 0.8mg/L, and the examination of each sample was repeated three times to ensure its accuracy. Results and the 0.2 mg/L concentration were the detection limit value of the RGB method with the smartphone because it is the lowest value that has been detected by this method in practice, as in Figure 5.

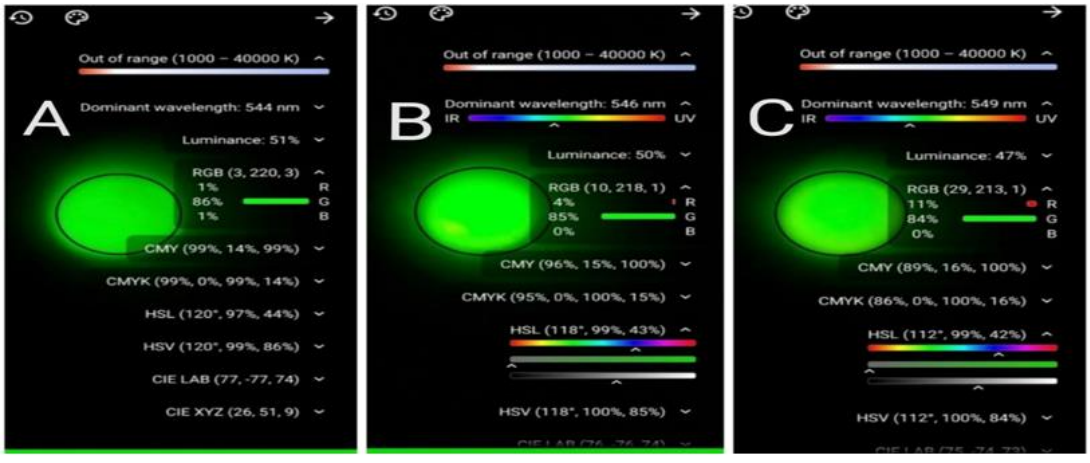

Fig. 5. The images taken to study the concentrations of the detection limit, (a) Image of a concentration of (0.2 mg/L). (b) Image of a concentration of (0.4mg/L). (c) Image of a concentration of (0.8mg/L)

3.5. Smartphone Standard Calibration Curve for Colour Density Method

Under the optimal conditions studied, the calibration curve was obtained for the concentration of iron (II) in the

samples. Figure (6) is a graph showing the linearity of the application of (Beer Lambert's Law) within the range (1-8 mg/L) between absorbance and iron II concentrations as shown in the Table (2). The linear graph has a correlation coefficient (R^2) equal to (0.999), and the value of the relative standard deviation coefficient (RSD %) for the concentration of (4) mg/L for eight repeated assays is (0.6%), and the value of recovery% is equal to (101.5%) Table 3.

Table 2
The results of the calibration curve for RGB method

NO	Concentration mg/L	G	Absorbance
0	0	220	0
1	1	208	0.0243
2	2	197	0.0479
3	3	185	0.0752
4	4	175	0.0993
5	6	157	0.1465
6	8	141	0.1932

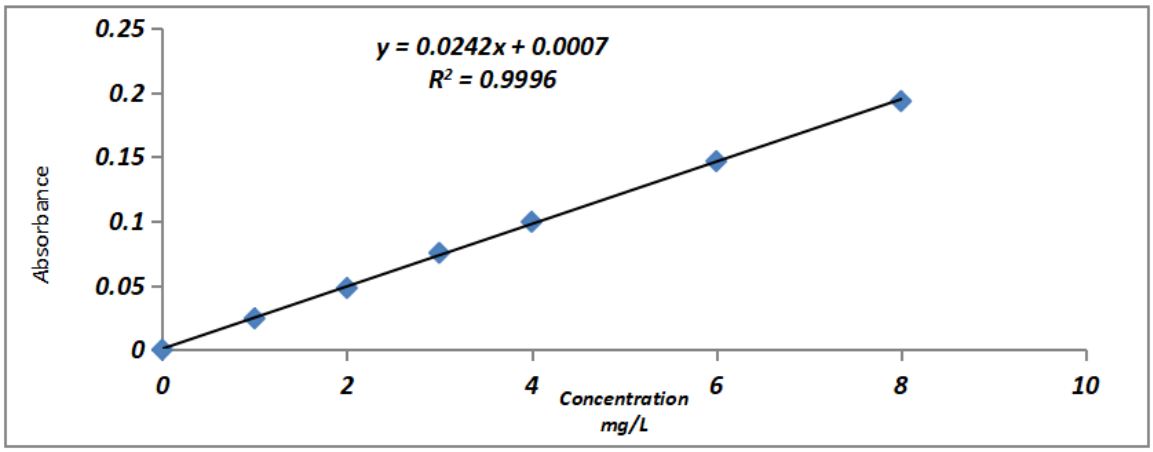

Fig. 6. Chart for calibrating the concentrations of iron (II) with absorbance using the RGB method

Table 3
Optimum Conditions for RGB Method

Analytical values	Values
Limits of Applicability of the (Beer-Lambert) Law (mg/L)	8-Jan
Detection limit (mg/L)	0.2
(Recovery%) for a concentration of (4 mg/L) for 10 assays	101.50%
(RSD%) for concentration (4 mg/L) for 10 assays	0.60%
Correlation coefficient (R2)	0.999
(Slope)	0.0242

3.6. Accuracy of RGB Method

In order to demonstrate the accuracy and sensitivity of the RGB method in determining the concentration of iron (II) using a smartphone. Analytical sample number (2) was prepared with a concentration of (5) mg/L and a concentration of (7) mg/L, and the samples were measured by the traditional method using the (spectrophotometer) and the chromatic density method (RGB). The average recovery was for three Measurements in the range (101.4 – 100.42 %). Good results were obtained, as shown in Table 4, which clearly indicates that RGB method is very suitable as a new method for the determination of iron in water.

Table 4
The results of the examination of analytical samples by the traditional method and (RGB) method with a smartphone

Analytical samples mg/L	Traditional Method mg/L	*RGB Method mg/L	RSD% Traditional Method	RSD% (RGB) Method	Recovery% Traditional method	Recovery % (RGB) Method
5	4.8	5.09	0.9	0.6	96%	101.4 %
7	6.8	7.03	0.8	0.5	97.42%	100.4 %

* The average of three assays was extracted for both methods.

4. Conclusion

Designing a room in the form of a plastic box (black acrylic), opaque, on which a smartphone case is installed, and inside it a flow cell and a light reflecting mirror, a green filter complementing the red colour, and a micro switch. Iron (II) in water was measured in a new way using the colour density (RGB) of a smartphone. Considering the RGB method for measuring iron in water, as a new method compared to traditional measurement methods, it is

characterized by being an easy-to-use and low-cost method, and it can be used in work sites far from the laboratory.

Competing Interests

The authors have declared that no competing interests exist.

References

Audet, Y., & Chapman, G. H. (2001, October). Design of a self-correcting active pixel sensor. In Proceedings 2001 IEEE International Symposium on Defect and Fault Tolerance in VLSI Systems (pp. 18-26). IEEE. https://doi.org/10.1109/DFTVS.2001.966748

Bigas, M., Cabruja, E., Forest, J., & Salvi, J. (2006). Review of CMOS image sensors. Microelectronics Journal, 37(5), 433-451. https://doi.org/10.1016/j.mejo.2005.07.002

Christodouleas, D. C., Nemiroski, A., Kumar, A. A., & Whitesides, G. M. (2015). Broadly available imaging devices enable high-quality low-cost photometry. Analytical chemistry, 87(18), 9170-9178. https://doi.org/10.1021/acs.analchem.5b01612

Coulombe, J., Sawan, M., & Wang, C. (2000, May). Variable resolution CMOS current mode active pixel sensor. In 2000 IEEE International Symposium on Circuits and Systems (ISCAS) (Vol. 2, pp. 293-296). IEEE. https://doi.org/10.1109/ISCAS.2000.856319

Croft, D. (1999). Cmos image sensors compete for low-light tasks. Laser Focus World, 35(1), 135-140.

Durini, D. (Ed.). (2019). High performance silicon imaging: fundamentals and applications of cmos and ccd sensors. Woodhead Publishing.

El Gamal, A., Eltoukhy, H., & Sensors, C. I. (2005). IEEE Circuits& Device Magazine, May. June6—20.

Fossum, E., & Krymski, A. (2000, July). High speed CMOS imaging. In 2000 Digest of the LEOS Summer Topical Meetings. Electronic-Enhanced Optics. Optical Sensing in Semiconductor Manufacturing. Electro-Optics in Space. Broadband Optical Networks (Cat. No. 00TH8497) (pp. I3-I4). IEEE. https://doi.org/10.1109/LEOSST.2000.869673

Ginhac, D. (2014). Smart cameras on a chip: using complementary metal-oxide-semiconductor (CMOS) image sensors to create smart vision chips. In High Performance Silicon Imaging (pp. 165-188). Woodhead Publishing. https://doi.org/10.1533/9780857097521.1.165

Goy, J., Courtois, B., Karam, J. M., & Pressecq, F. (2001). Design of an APS CMOS image sensor for low light level applications using standard CMOS technology. Analog Integrated Circuits and Signal Processing, 29(1), 95-104. https://doi.org/10.1023/A:1011286415014

Haris, D. C. (2003). Determination of Iron with 1, 10-Phenanthroline. Quantitative Chemical Analysis, 6th ed., WH Freeman & Company, New York, 258-261.

Iqbal, Z., & Eriksson, M. (2013). Classification and quantitative optical analysis of liquid and solid samples using a mobile phone as illumination source and detector. Sensors and Actuators B: Chemical, 185, 354-362. https://doi.org/10.1016/j.snb.2013.05.009

Koren, I., Chapman, G., & Koren, Z. (2000, October). A self-correcting active pixel camera. In Proceedings IEEE International Symposium on Defect and Fault Tolerance in VLSI Systems (pp. 56-64). IEEE. https://doi.org/10.1109/DFTVS.2000.886974

Levin, A., & Stevens, P. E. (2014). Summary of KDIGO 2012 CKD Guideline: behind the scenes, need for guidance, and a framework for moving forward. Kidney International, 85(1), 49-61. https://doi.org/10.1038/ki.2013.444

Marczenko, Z., & Balcerzak, M. (2000). Separation, preconcentration and spectrophotometry in inorganic analysis. Elsevier.

Roda, A., Michelini, E., Zangheri, M., Di Fusco, M., Calabria, D., & Simoni, P. (2016). Smartphone-based biosensors: A critical review and perspectives. TrAC Trends in Analytical Chemistry, 79, 317-325. https://doi.org/10.1016/j.trac.2015.10.019

Shcherback, I., & Yadid-Pecht, O. (2003). Photoresponse analysis and pixel shape optimization for CMOS active pixel sensors. IEEE Transactions on Electron Devices, 50(1), 12-18. https://doi.org/10.1109/TED.2002.806966

Zhang, W., Chan, M., Wang, H., & Ko, P. K. (1999, October). Building hybrid active pixels for CMOS imager on SOI substrate. In 1999 IEEE International SOI Conference. Proceedings (Cat. No. 99CH36345) (pp. 102-103). IEEE. https://doi.org/10.1109/SOI.1999.819873

Zhou, Z., Pain, B., & Fossum, E. (1998, February). A CMOS imager with on-chip variable resolution for light-adaptive imaging. In 1998 IEEE International Solid-State Circuits Conference. Digest of Technical Papers, ISSCC. First Edition (Cat. No. 98CH36156) (pp. 174-175). IEEE. https://doi.org/10.1109/ISSCC.1998.672422